

Development and performance analysis of PCL/silica nanocomposites for bone regeneration

Luigi Calandrelli · Marco Annunziata ·
Fulvio Della Ragione · Paola Laurienzo ·
Mario Malinconico · Adriana Oliva

Received: 20 November 2009 / Accepted: 31 August 2010 / Published online: 7 October 2010
© Springer Science+Business Media, LLC 2010

Abstract In the present article, several developments of biocomposites containing silica nanoparticles intended for bone regeneration are reported. Nanocomposites of poly(ϵ -caprolactone) (PCL) and silica, in which either the silica nanoparticles or the PCL have been modified in order to improve interfacial adhesion through chemical graft between the phases are hereafter described. The composites are characterized with respect to their chemical–physical and mechanical properties. Their biocompatibility and capacity to induce the osteoblastic phenotype in human bone marrow mesenchymal stem cells have been assessed.

1 Introduction

Osteoinductive materials are strongly searched in reconstructive surgery. Polymer based composites are ideal candidate, as they couple the ease of processing of polymers (by melt or by injection and hardening) with the mechanical reinforcement of fillers, once interfacial adhesion is assured. In particular, nanocomposites have been largely studied for their superior mechanical characteristics. Natural bone itself

is a true nanocomposite composed mainly of HA nanocrystallites in the collagen-rich organic matrix [1, 2]; thereby choosing a composite containing either HA nanocrystals or a component that induce HA nanocrystals formation as a bone graft material is an added advantage, as it mimics the bone components. Nanocrystalline HA promotes osteoblast cells adhesion, differentiation, and proliferation, osteointegration and deposition of calcium containing minerals on its surface better than microcrystalline HA, thus enhancing the formation of new bone tissue within a short period [3–5].

Silica, the mineral of which sand is made, is generally inert in the body and can be modified easily using a variety of well-established chemical reactions. As such, researchers have considered silica an ideal candidate material from which to create multifunctional nanoparticles. Several examples of nanocomposites based on acrylic matrices containing silica nanoparticles as bioactive filler for bone cement [6, 7] and resin for dental applications [8, 9] have been reported. The authors always observed high mechanical properties in addition to crystalline apatite formation on implants in simulated body fluid (SBF), proving that silica nanoparticles act as a nucleation site for several salts, as calcium phosphates, that promote formation of HA in in vivo simulating conditions. Formation of an apatite layer and favourable mechanical properties were also observed on PCL/silica nanocomposites [10–12].

To improve the interface with the organic matrix, silica based nanoparticles can be chemically or physically modified [13]. The silanization method is widely used for chemical modification; as a conventional silanization reagent, trimethoxysilylpropyldiethylenetriamine (DETA) has been reported to introduce amine groups onto the surfaces of silica nanoparticles [14]. Similarly, trimethoxysilanePEG and trifluoroethylene PEG silane have been

L. Calandrelli (✉) · P. Laurienzo · M. Malinconico
Institute of Polymers Chemistry and Technology, CNR,
Via Campi Flegrei 34, 80078 Pozzuoli, Naples, Italy
e-mail: luigi.calandrelli@ictp.cnr.it

F. Della Ragione · A. Oliva
Department of Biochemistry and Biophysics,
Faculty of Medicine, Second University of Naples,
Via L. De Crescchio 7, Naples, Italy

M. Annunziata
Department of Odontostomatological, Orthodontic and Surgical
Disciplines, Second University of Naples, Via L. De Crescchio 6,
Naples, Italy

shown to link to silica based nanospheres and introduce PEG molecules onto the nanosphere surface [13, 15–17]. Vinyl modified silica nanoparticles have been photopolymerized with acrylic monomers to develop polymethacrylate-silica hybrid/nanocomposite dental materials characterized by low volume shrinkage [18].

Bone marrow is a complex cellular array of stem cells of both hematopoietic and nonhematopoietic lineages. In 1987 Friedenstein et al. showed that a specific set of cells (colony forming unit fibroblasts, CFU-F) present in bone marrow can differentiate into different cell types, including osteoblasts [19]. These cells, referred to as mesenchymal stem cells or marrow stromal cells (MSCs), have a great capacity of self-renewal and multipotency. MSCs, indeed, can give rise to precursors for bone, cartilage, adipose tissue, tendon, muscle, and marrow stroma [20, 21]. In addition, MSCs have been demonstrated to be capable to differentiate into cardiomyocytes, astrocytes and neurons [22–24]. A number of studies on MSCs have demonstrated the great plasticity of these cells and that their fate strictly depends on various environmental signals [25, 26].

An ideal bone tissue engineering strategy implies the use of autologous bone marrow MSCs. A serious drawback to this approach is represented by the low number of MSCs in bone marrow. In this respect, the utilization of own platelet-rich plasma, that is a rich source of a number of growth factors essential in the modulation of the wound-healing process, can be a method for the rapid *ex vivo* expansion of MSCs before their clinical application, avoiding the use of heterologous human- or animal-derived growth supplements as well as expensive recombinant growth factors [27].

In the present article, several recent developments of bio-nanocomposites intended for bone regeneration based on poly(ϵ -caprolactone) (PCL) and silica nanoparticles are reported. To improve the interface, both PCL and silica nanoparticles surface have been modified with the aim to chemically graft the nanoparticles to the polymer matrix. The nanocomposites have been characterized with respect to their chemical–physical and mechanical properties. Their biocompatibility and capacity to induce the osteoblastic phenotype in human bone marrow mesenchymal stem cells have been assessed. Furthermore, materials obtained by blending PCL/silica nanocomposites with poly(L-lactide) (PLLA) have been prepared and tested regards to their biological properties. PLLA has been widely reported as material for bone regeneration [28–30], due to its mechanical properties and biodegradation rate compatible with bone regeneration, so a blending of the two polymers is expected to give better performances in terms of mechanical characteristics as well as biological response.

2 Experimental

2.1 Materials

Poly- ϵ -caprolactone (PCL) CAPA[®] 650, molecular weight 50,000 m.a.u., was a gentle gift from Solvay (Italy).

Poly(L-lactide) (PLLA—Resomer L206S), is a product of Boehringer-Ingelheim.

Nanostructured silica Aerosil[®] 90, as well as functionalized nanostructured silica Aerosil[®] R7200, were a kind gift from Degussa, Germany (dimensions comprised between 100 and 200 nm). The nanoparticles were prepared following the Stöber method [30].

Dibenzoylperoxide (DBPO) is a Sigma-Aldrich product.

Glycidylmethacrylate (GMA) and butylmethacrylate (BMA) are Fluka reagent grade products.

All cell culture biologics were purchased from (Life Technologies, MD, USA), and all chemicals were from Sigma Chemical Co (St. Louis, MO, USA) when not otherwise specified.

Murine fibroblasts NIH 3T3 were from ATCC (LGC Milano).

2.2 Preparation of nanocomposites

Nanocomposites based on plain PCL with a percentage of not functionalized silica of 1, 3 and 5% have been prepared. The silica employed was Aerosil[®] 90 (A90). At first three different mixtures have been prepared in the following proportions:

- PCL/A90 1% = 49.5 g of PCL + 0.5 g of A90
- PCL/A90 3% = 48.5 g of PCL + 1.5 g of A90
- PCL/A90 5% = 47.5 g of PCL + 2.5 g of A90

The preparation of the material has been made in a static mixer type Brabender (Rheocord) to a temperature of 100°C for an overall time of 20 min and at a rate of, 8 rpm for the first 10 min and then 32 rpm for the remaining time. 1.5 g of the material thus obtained have been compression moulded to a temperature of 100°C for 3 min and to a pressure of 5 kg/cm², in order to obtain a film having the dimensions of approximately 10 × 10 cm and a thickness between 80 and 100 μ m for biological analysis. Around 4 g of material have been compression moulded in the same experimental conditions within a frame 1 mm thick to obtain samples for tensile tests.

2.2.1 Functionalized nanocomposites

For allowing a direct comparison, functionalized nanocomposites having the same percentages of nanosilica, that is, 1, 3 and 5%, have been realized. It has been employed the functionalized silica Aerosil[®] R7200 (AR72) with a vinyl

end group. Moreover the PCL has been in situ functionalized with glycidylmethacrylate (GMA) using dibenzoylperoxide (DBPO) as radical source. DBPO was previously dissolved in GMA. The three different nanocomposites have been prepared in the following proportions:

- PCL-g-(GMA-AR72 1%) = 49.5 g of PCL + 0.5 g of AR72 + 0.495 g DBPO + 4.95 g of GMA
- PCL-g-(GMA-AR72 3%) = 48.5 g of PCL + 1.5 g of AR72 + 0.485 g DBPO + 4.85 g of GMA
- PCL-g-(GMA-AR72 5%) = 47.5 g of PCL + 2.5 g of AR72 + 0.475 g DBPO + 4.75 g of GMA

The preparation has been made in a static mixer type Brabender (Rheocord) at a temperature of 100°C; initially, PCL and GMA/DBPO are mixed for 10 min at a rate of 8 rpm in order to obtain the formation of the GMA grafted PCL, then AR72 is added and the reaction goes on for further 10 min to copolymerize the functionalized silica on the PCL-g-GMA growing chains (reactive mixing) progressively increasing the number of turns from 8 to 32 rpm. Also for these materials films have been prepared as previously described. A nanocomposite with 3% of silica in which GMA has been replaced with BMA has been prepared under the same experimental conditions.

As reference and control materials also the following samples have been prepared:

- PCL functionalized with 1% GMA (PCL-g-GMA)
- PCL functionalized with GMA + 1% not functionalized silica A90 (PCL-g-GMA/A90 1%)

2.2.2 Nanocomposites/PLLA blends

Blends between the nanocomposite PCL-g-(BMA-AR72) with 3% of silica and PLLA have been prepared by a solution method, dissolving the nanocomposite and the PLLA at different compositions in chloroform (1.5 g of total material in 10 cc of chloroform). The solution is then poured in a Petri dish and the solvent is let to evaporate at room temperature. The obtained cast film is finally dried under vacuum overnight. Blends of compositions 70/30, 50/50 and 30/70 by weight have been prepared.

2.3 Differential thermal analysis

Differential thermal analysis (DSC) on polymer matrix (PCL) has been carried out using the following thermal cycle: heating of the sample from 30 to 180°C at a scanning speed of 10°C/min then cooling to –100°C to the scanning speed of 10°C/min and successive heating till 180°C to the same scanning speed. The nanocomposites have been subjected to the same thermal cycle. The calorimeter used was Mettler DSC 30.

2.4 Mechanical tests

Tensile mechanical tests have been performed on samples in the form of dog's bone just like the norm prescribes, and tested in traction in order to obtain relevant mechanical parameters. The tests have been carried out on a Instron dynamometer model 4505 at room temperature with a traction speed of 10 mm/s.

2.5 Scanning electron microscopy

The morphology of the materials has been evaluated examining the fracture surfaces by scanning electron microscopy (SEM). The samples were fractured in liquid nitrogen, mounted on a support and metallized with a Au/Pd alloy. The microscope used was a Philips XL 20.

2.6 Elution test

The samples, in form of thin layers, were first sterilized in a steam autoclave and then placed in a suitable ratio weight/volume of Dulbecco's modified Eagle's medium (0.1 g/ml medium) containing penicillin (100 units/ml), streptomycin (100 µg/ml) and fungizone (1.2 µg/ml), and left under stirring at room temperature either for 24 or for 48 h. The corresponding extracts were added, as such (100%) or diluted 1:1 (50%), to confluent 3T3 cells, that had been plated 2 days before in multiwell-12. The cultures were incubated at 37°C in a 5% CO₂ humidified atmosphere and cell vitality at 24 and 48 h was assessed by MTT test.

2.7 Preparation and characterization of bone marrow MSCs

The preparation of MSCs was performed employing heparinized human bone marrow from healthy volunteers, after informed consent, following the method of Friedenstein et al. with some modifications [27, 31]. Taking into account that a number of factors, as the donor-to-donor variability, age, gender, etc., might affect the biological response, four different MSCs populations were obtained in order to enhance data reliability.

Briefly, the bone marrow sample was diluted 1:5 with Opti-MEM (Life Technologies, MD, USA), containing 10% fetal calf serum (FCS), penicillin 100 units/ml, streptomycin 100 µg/ml and sodium ascorbate 50 µg/ml (growth medium), placed in 100 mm polystyrene dishes and incubated at 37°C in a 5% CO₂ humidified atmosphere.

After 48 h, the medium was collected and centrifuged at 800 rpm. Half of the supernatant (conditioned medium, CM) was aspirated, added with an equal volume of fresh medium and placed in the first plate. The medium remaining in the tube was used to resuspend the cellular

pellet and, after the addition of an equivalent volume of fresh culture medium, the entire cellular suspension was plated in a second dish. The day after, also the medium of the second plate was centrifuged: the pellet, containing all non-adherent cellular elements, was discarded while the corresponding CM was added again to the dish.

In 2–4 days, several foci of adherent spindle-like cells started to appear and to develop until to colonize the whole dish surface in the following 2 weeks. During this period fresh medium was added every 3 days, each time leaving one half of the old medium. After the reaching of the confluence, cells were trypsinized and amplified always diluting the conditioned medium.

MSCs were analyzed by flow cytometry using a wide panel of monoclonal antibodies. The cells expressed specific surface markers, such as CD13, CD29, CD44, CD105, CD166, and were negative for hematopoietic cell markers CD14, CD34 and CD45.

Cultures between the 3rd and 5th passage were used in our experiments. The cells harvested from each donor were kept separately and not pooled with other preparations.

In presence of osteogenic inducers, the stromal cells go through a complex series of events, at the end of which the multipotent cells become terminally differentiated. Alkaline phosphatase and osteocalcin are phenotypic markers for early-stage differentiated and terminally differentiated osteoblasts, respectively.

2.8 Direct contact test

The samples, in form of discs (21 mm diameter and 0.1 mm thickness), were attached with biological silicone (NuSil Silicone Technology, CA, USA) to the bottom of 12-well plates and sterilized 24 h with PBS containing penicillin (1000 units/ml), streptomycin (1000 µg/ml) and fungizone (12.5 µg/ml) at 37°C in a 5% CO₂ humidified atmosphere. The materials were then placed in Opti-MEM containing antibiotics and fungizone (at concentrations 10-fold lower than those indicated above), 10% FCS and 50 µg/ml sodium ascorbate (complete medium) and kept in the incubator overnight before plating the cells.

MSCs were seeded on discs at a density of 15,000 cells/cm² in complete culture medium and incubated for up to 2 weeks at 37°C in a 5% CO₂ humidified atmosphere. Cell adhesion and vitality, as well as alkaline phosphatase activity and osteocalcin levels were evaluated.

2.9 MTT test

The MTT assay is a very simple and useful tool for evaluating cell vitality and proliferation. The key component is 3-(4,5-dimethylthiazol-2-yl)-2,5-diphenyltetrazolium bromide (MTT). Mitochondrial dehydrogenases of living cells

reduced the tetrazolium ring, yielding a blue formazan product, which was measured spectrophotometrically. The amount of formazan produced is proportional to the number of viable cells present. MTT (5 mg/ml in DMEM without phenol red) was added to the wells in an amount equivalent to 10% of the culture medium. After an incubation of 4 h at 37°C, the liquid was aspirated and the insoluble formazan produced was dissolved in isopropanol. The optical densities were measured at 570 nm, subtracting background absorbance determined at 690 nm.

2.10 Alkaline phosphatase assay

After the removal of the medium, the wells were rinsed with 20 mM TRIS HCl-0.5 M NaCl, pH 7.4 (TBS) and the cells were solubilized with lysis buffer, that is TBS containing DTT (0.5 mM), PMSF (0.5 mM) and Triton X-100 (0.25%). After 30 min in ice, the cell lysates were centrifuged at 12,000×g for 5 min, and the supernatants assayed for alkaline phosphatase activity. The protein concentration was determined using the protein assay kit (Bio-Rad Laboratories, CA, USA), according to the method of Bradford.

AP activity was determined by measuring the release of *p*-nitrophenol from disodium *p*-nitrophenyl phosphate (PNPP). The reaction mixture contained 0.1 M diethanolamine buffer, pH 10.5, 0.5 mM MgCl₂ and 12 mM PNPP in a final volume of 0.5 ml. The reaction was initiated by the addition of the cell extract and the mixture was incubated at 37°C for 30 min. The reaction was stopped by adding 0.5 ml of 0.5 M NaOH and the absorbance was determined spectrophotometrically at 405 nm. The AP activity was normalized to the protein content and expressed as units/mg protein, where one unit was defined as the amount of enzyme that hydrolyzes 1 nmol of PNPP/min under the specified conditions.

2.11 Osteocalcin synthesis

To evaluate osteocalcin synthesis, confluent cultures grown on the different surfaces for 2 weeks were incubated in FCS-free Opti-MEM in presence of 0.1% bovine serum albumin and 100 nM 1,25-dihydroxycholecalciferol for 48 h. The levels of polypeptide secreted in the medium were measured by means of an immunoenzymatic assay (Biosource International, Camarillo, CA, USA) that utilizes monoclonal highly specific antibodies and a peroxidase as conjugated enzyme. The amount of osteocalcin was calculated in ng/ml and then normalized to the protein content.

2.12 Statistical analysis

All the experiments were performed in triplicate on at least two different cell preparations. Data are expressed as the

mean \pm standard deviation (SD) of values. The means of each experimental group were compared by one-way analysis of variance (ANOVA) followed by Tukey's post hoc test. Differences at $p < 0.05$ were considered to be statistically significant.

3 Results and discussion

Nanocomposites obtained simply by mixing unmodified PCL and unmodified silica nanoparticles, A90 (see Experimental), in percentage of silica of 1, 3 and 5% have been prepared and characterized before their functionalization. The scope of this preliminary study was to verify if in the absence of specific interfacial interactions, but simply with the addition of a nanometric filler to the polymer matrix, the physical and mechanical chemical properties of the PCL could improve. Calorimetric analysis (DSC) of the PCL evidences that the presence of the nanosilica has not caused any variation of the transition temperatures (T of fusion, T of crystallization and T of glass transition). Also the thermal stability of composites did not seem to be influenced from the presence of the silica.

The tensile tests carried out in order to estimate parameters such as stress at break, Young's modulus and extensibility, indicate that increasing the percentage of silica leads to a corresponding increase of the modulus and a diminution of the extensibility (Table 1). This to demonstrate that it is possible to increase the structural properties of the PCL without depressing in considerable measure the plastic properties of the material.

3.1 Chemical modification and characterization of nanocomposites

It is found in literature that in presence of specific interfacial interactions between matrix and nano-reinforcement, it is possible to exalt the performances of the nanocomposites. In order to improve the interfacial adhesion between the matrix and the nanoparticles, to promote the formation of a reactive interphase and to increase the hydrophilicity, opportune chemical modifications have been carried out either on the polyester chain or on the surface of the nanoparticles. In particular, the PCL has been functionalized introducing in

chain approximately 10% by weight of glycidylmethacrylate (GMA). In the first step, GMA is grafted onto PCL chains through a radical mechanism with dibenzoylperoxide (DBPO) as initiator, at $T = 100^\circ\text{C}$. After 10 min of reaction, nanoparticles of silica, characterized by the presence on the surface of vinyl groups (Aerosil[®] R7200), hence able to be linked to the PCL through copolymerization with GMA during the radical homopolymerization, have been added in the Rheocord chamber and the mixing was continued at 100°C for further 10 min, gradually increasing the rate from 8 to 32 rpm. In Fig. 1 we show the sequence of the reactions that leads to the formation of the functionalized nanocomposites.

The functionalized nanocomposites (containing 1, 3 or 5% of nanoparticles, as well as previously not functionalized nanocomposites) have not demonstrated substantial and meaningful differences by thermal analysis compared to the results obtained for not functionalized nanocomposites.

Tensile tests have been carried out in order to characterize the mechanical behaviour of the materials. Results are reported in Table 2. As it is possible to observe, the presence of the nanoparticles of silica generates an increment of the Young's modulus. In turn, such increment results to be more meaningful once the chemical modifications so far illustrated are introduced (see Table 1 for a comparison). Also in this case, the variations recorded are in agreement with the content of nanoreinforcement that acts hence as a rigid filler, hardening the system.

Moreover, we notice from Table 2 that the increment of the Young's modulus, although significant when increasing the percentage of nanosilica, turns out to be nearly equal in the percentage of the 3 and 5% thus demonstrating that the increase of the total surface of the nanoparticles determines the impossibility for the polymer matrix to coat it all. As a consequence, high percentages of nanosilica caused the birth of structural defects with worsening of the mechanical properties or at least an invariance of properties. Tensile tests have been carried out also on the nanocomposite in which the functionalization regards only PCL (PCL-g-GMA/A90 1%) and on the corresponding not functionalized nanocomposite (PCL/A90 1%). In the direct comparison we notice that the single chemical modification of the PCL phase itself determines an increment of the mechanical properties that approach those of the functionalized

Table 1 Mechanical parameters of plain PCL and of PCL/A90 silica nanocomposites

PCL/A90	Stress at break (MPa)	Young's modulus (MPa)	Elongation at break (%)
100/0	44 \pm 2	380 \pm 23	1500 \pm 210
99/1 (1%)	40 \pm 4	430 \pm 12	1366 \pm 173
97/3 (3%)	37 \pm 3	500 \pm 14**	1400 \pm 113
95/5 (5%)	37 \pm 4	520 \pm 11**	1300 \pm 138

** $p < 0.01$ versus 100/0

Fig. 1 The sequence of reactions which lead to the formation of functionalized nanocomposites

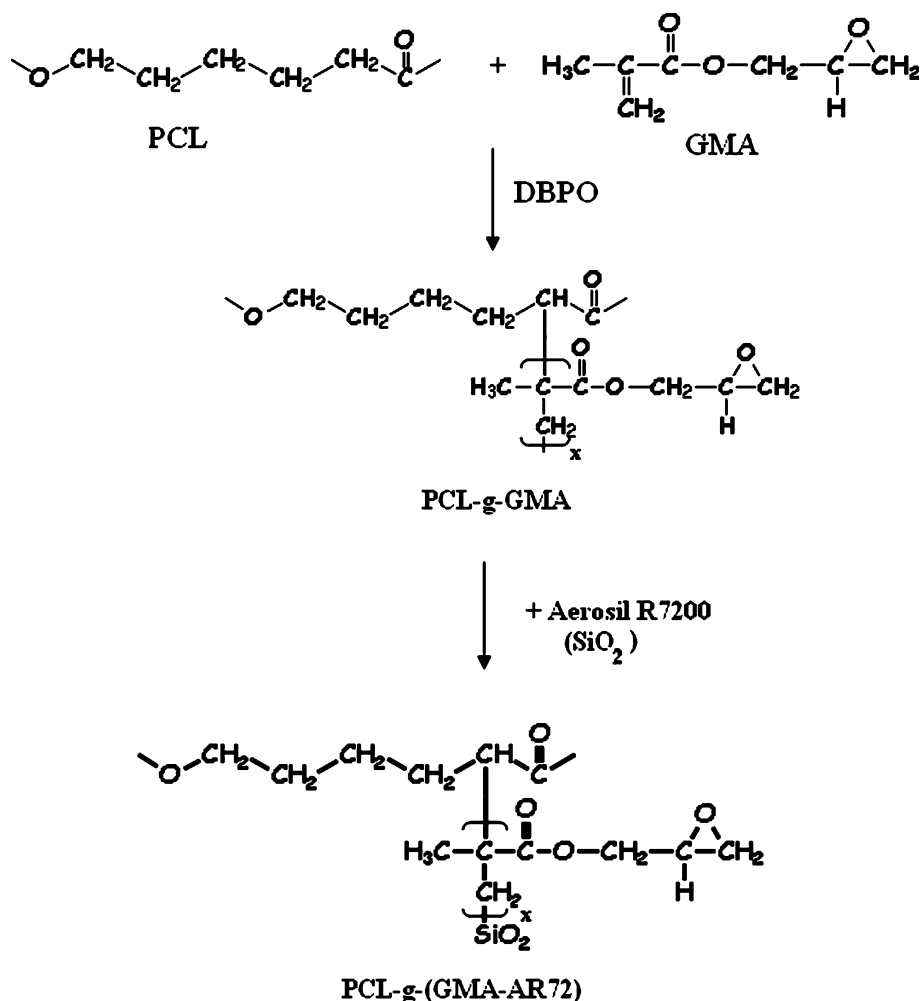


Table 2 Mechanical parameters of plain PCL and of PCL-g-(GMA-AR72) functionalised silica nanocomposites

Sample (silica %)	Stress at break (MPa)	Young's modulus (MPa)	Elongation at break (%)
PCL	44 ± 2	380 ± 23	1500 ± 210
PCL-g-(GMA-AR72) 1%	24 ± 3	509 ± 16**	563 ± 161
PCL-g-(GMA-AR72) 3%	19 ± 4	566 ± 17**	443 ± 28
PCL-g-(GMA-AR72) 5%	20 ± 3	563 ± 18**	510 ± 59
PCL-g-GMA/A90 1%	22 ± 3	517 ± 27**	577 ± 91
PCL/A90 1%	40 ± 4	430 ± 12	1366 ± 173

** $p < 0.01$ versus both PCL and PCL/A90 1%

nanocomposite, while PCL/A90 1% has slightly better properties compared to neat PCL but clearly inferior to those of the PCL-g-GMA/A90 1% nanocomposite.

3.2 Morphologic analysis (SEM)

Fracture surfaces of not functionalized as well as functionalized systems have been observed with a Scanning Electron Microscope (SEM). Nanocomposites between not functionalized PCL and not functionalized silica (PCL/A90

1%, PCL/A90 3%, PCL/A90 5%, Fig. 2), show, at least till 3%, a good dispersion of the nanofillers in the polymer matrix, but an insufficient interfacial adhesion is found. At 5% content, aggregation of the nanofillers begins to be evident. The nanocomposite prepared with the functionalized PCL and the not functionalized silica (PCL-g-GMA/A90 1%) shows a morphology significantly different from the analogous not functionalized system (PCL/A90 1%) (Fig. 3), characterized by an elevated interconnection between the phases evidenced from the extensive covering

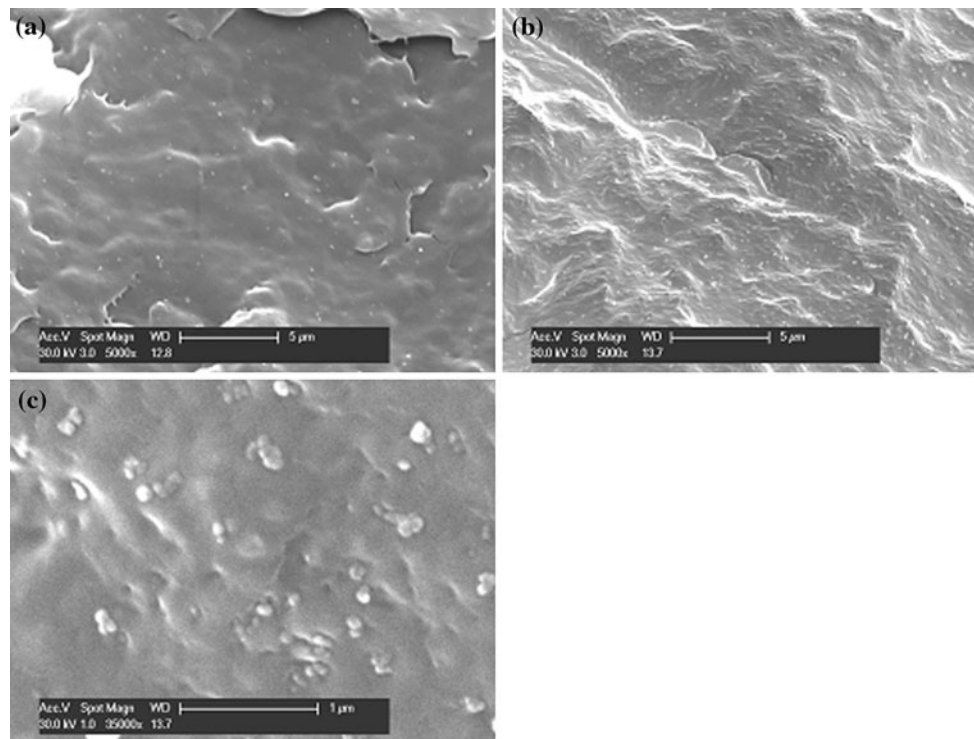


Fig. 2 SEM micrographs of: **a** PCL/A90 1%, **b** PCL/A90 3%, **c** PCL/A90 5% nanocomposites

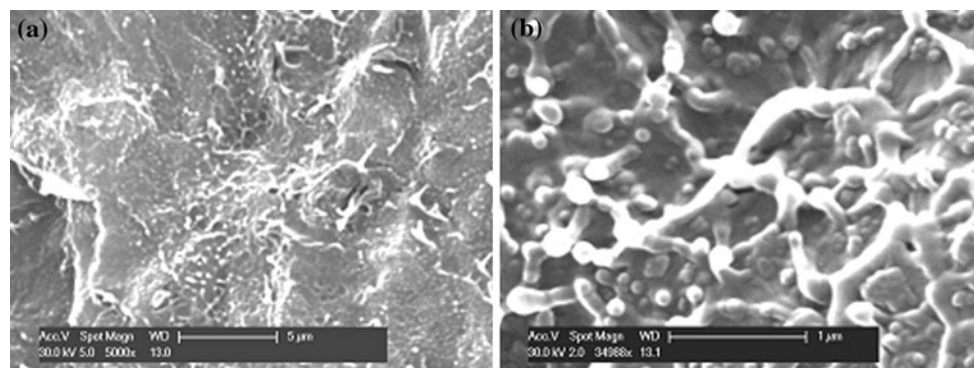


Fig. 3 SEM micrographs of PCL-g-GMA/A90 1% at different magnifications

of the nanofillers with the polymer matrix. In Fig. 3b the interconnection is better appreciated. These phenomena boast in the nanocomposites where both the components are functionalized (PCL-g-(GMA-AR72) 1%, PCL-g-(GMA-AR72) 3%, PCL-g-(GMA-AR72) 5%; Fig. 4). In fact in the mixture at 1% a greater adhesion of the nanofiller to the polymer matrix is observed. The phenomenon then becomes evident in the nanocomposite with 3% of functionalized silica and seems to become stabilized, without great changes, at 5% content. It is interesting to emphasize that, as a result of this covering of the nanofillers with the matrix, for the same composition the surface of the functionalized system seems much more covered from nanofillers than the analogous mixture not made compatible.

As above mentioned, the functionalization of the PCL with glycidylmethacrylate (GMA) was required to improve the hydrophilicity of the employed PCL. On the basis of preliminary biological results (see next paragraph), it appeared that the epoxy function could be responsible for a decreased adhesion of cells compared to PCL. GMA has been therefore replaced with butylmethacrylate (BMA). BMA is to be considered a monofunctional monomer as the only reactive group is the double bond, while GMA is a bifunctional acrylic with two reactive groups, namely the double bond and the epoxy group. In Fig. 5 we show the reactions that lead to the functionalization of the PCL with the BMA and the nanostructured silica. The preparation of the nanocomposites is the same as previously shown.

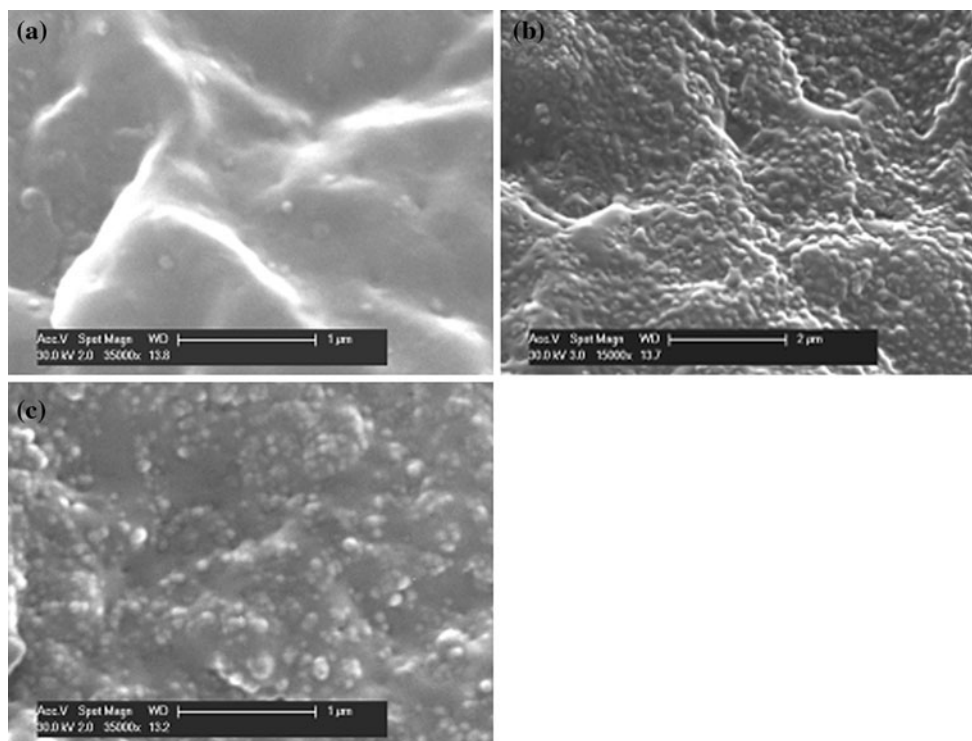


Fig. 4 SEM micrographs of: **a** (PCL-g-(GMA-AR72) 1%, **b** PCL-g-(GMA-AR72) 3%, **c** PCL-g-(GMA-AR72) 5%

Fig. 5 Preparation of PCL-g-(BMA-AR72) nanocomposite

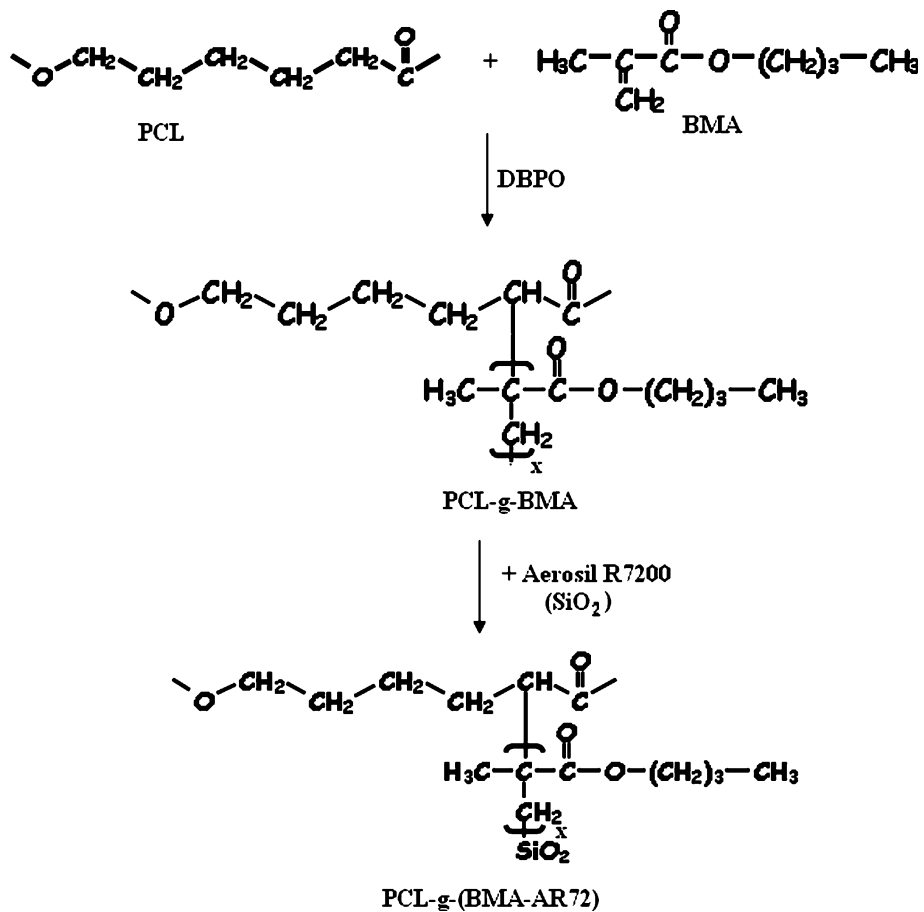


Table 3 Comparison of mechanical parameters of PCL-g-GMA, PCL-g-BMA, and their functionalized silica nanocomposites

Sample	Stress at break (MPa)	Young's modulus (MPa)	Elongation at break (%)
PCL-g-GMA	23 ± 7	510 ± 24	567 ± 68
PCL-g-(GMA-AR72) 3%	19 ± 4	566 ± 17*	443 ± 28*
PCL-g-BMA	21 ± 6	520 ± 22	559 ± 72
PCL-g-(BMA-AR72) 3%	22 ± 5	560 ± 19*	479 ± 58

* $p < 0.05$ versus both PCL-g-GMA and PCL-g-BMA

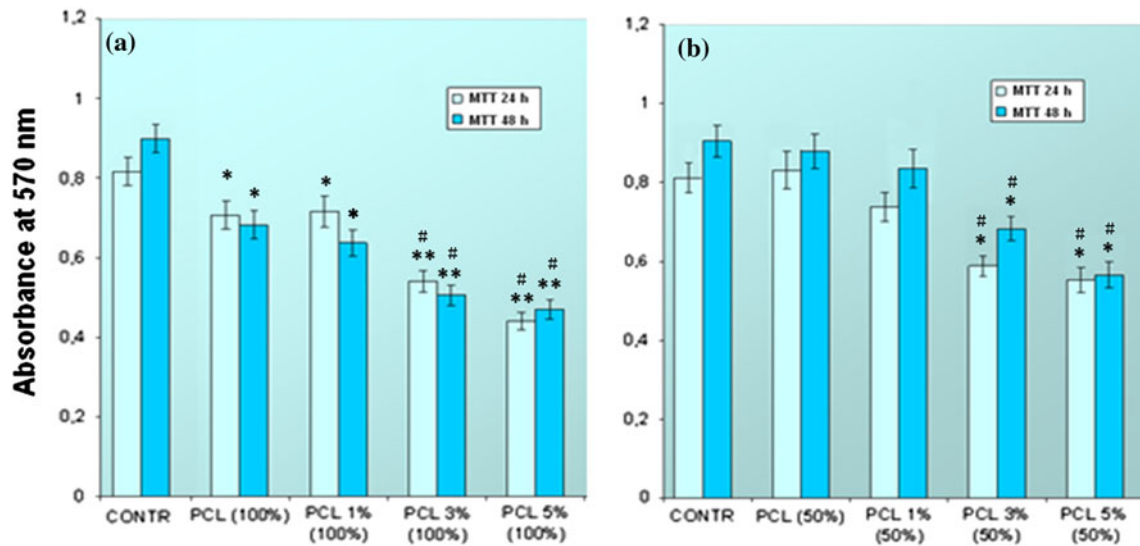


Fig. 6 MTT test on 3T3 fibroblasts incubated for 24 and 48 h in presence of either 100% (a) or 50% (b) not functionalized nanocomposites extracts. * $p < 0.05$ and ** $p < 0.01$ versus CONTR; # $p < 0.05$ versus PCL

As for the previously described system, nanocomposites with a percentage of 3% by weight were prepared and compared to pure PCL and pure PCL-g-BMA. Mechanical tensile tests have been performed in view of getting a comprehensive comparison of the properties with those collected on nanocomposites based on PCL-g-GMA, i.e. PCL-g-(GMA-AR72).

The results shown in Table 3 evidence an increase in Young modulus of the nanocomposite with respect to the related functionalized PCL, but the values are so close to each other that we can state no big difference in physical properties occurs when GMA group is replaced by BMA.

3.3 Biological evaluation

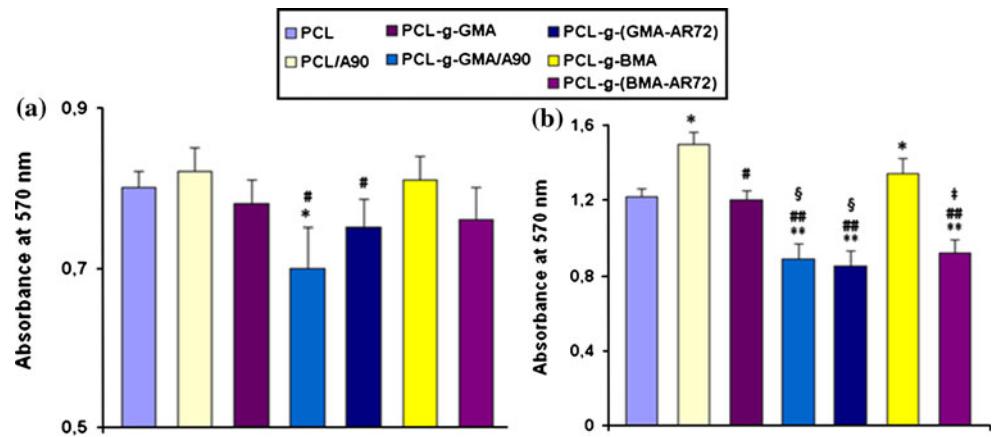
ISO 10993-5:2009 standards describe test methods that specify the incubation of cultured cells in contact with a device (direct contact test) and/or extracts of a device (elution test). In the direct contact method, the cells were cultured directly on the material under investigation and observed, for a period of days or weeks, in terms of morphological and functional features. Although the limits of all in vitro studies, including the present, are related to the

impossibility of reproducing the complex of the biological events that happen in vivo, nevertheless this type of approach can allow to investigate in detail the interaction between cells and implant surface. This initial phase is crucial, being the contact of cells with the biomaterial the basis for all the following events, including the expression of biochemical specific markers, as well as the deposition of an organized extracellular matrix and its mineralization.

We investigated in vitro the biocompatibility of the novel biocomposites as well as their capacity to induce the osteogenic differentiation of human bone marrow stromal cells. Cell proliferation and osteogenic differentiation were evaluated by MTT assay, alkaline phosphatase (AP) activity, osteocalcin (OC) content measurement.

Upstream to the in vitro studies with human cells, we analyzed the biocompatibility of the unmodified nanocomposite (PCL/A90) with different amount of silica nanoparticles (1, 3, and 5%) performing a set of elution tests in which murine cells (NIH-3T3) were subjected for 24 and 48 h to both 100 and 50% extracts of these materials (Fig. 6a and b, respectively). A certain toxicity at increasing percentages of silica was evident mostly with 100% extracts.

Fig. 7 MTT test carried out after plating 60,000 MSCs onto PCL (control) and its new derivatives and composites. **a** At 24 h, **b** after 7 days. * $p < 0.05$ and ** $p < 0.01$ versus PCL; # $p < 0.05$ and ### $p < 0.01$ versus PCL/A90; § $p < 0.05$ versus PCL-g-GMA; † $p < 0.05$ versus PCL-g-BMA



On the basis of this result and of the mechanical features of the PCL/A90 3% nanocomposite, which resembled the characteristics of bone tissue more than the others, we selected this composition as the starting material for the functionalized nanocomposites.

The following list reports all the materials tested on bone marrow stromal cells in a direct contact method:

- PCL
- PCL/A90 (not functionalized nanocomposite)
- PCL-g-GMA (functionalized PCL)
- PCL-g-GMA/A90 (functionalized PCL + nanosilica)
- PCL-g-(GMA-AR72) (functionalized PCL + functionalized nanosilica)
- PCL-g-BMA functionalized PCL)
- PCL-g-(BMA-AR72) (functionalized PCL + functionalized nanosilica)

The composite samples (21 mm diameter-0.1 mm thickness) were cut in semilunar form with a surface of 3.6 cm², attached with bioinert silicon on the bottom of polystyrene 12-multiwell plates (surface of each well = 4 cm²) and sterilized as indicated in the Experimental section. The 0.4-cm² area left uncovered from the sample was intended to allow the observation of the cells growing in the immediate proximity of the materials. In fact, they were opaque to microscopic observation due to their semicrystalline nature. Each material was tested at least in triplicate.

MSCs were seeded on discs at a density of 15,000 cells/cm² and incubated at 37°C in a 5% CO₂ humidified atmosphere. Cell vitality at 24 h were assessed by MTT test (Fig. 7a).

The reported values were directly related to the affinity of cells towards the materials. After 7-days of culture, MTT test was carried out again in order to assess cell growth on the various materials (Fig. 7b). The proliferation pattern reflected and overlapped that relative to adhesion of cells to the different discs, being PCL/A90 and PCL-g-BMA the composites that, more than others, had favoured the adhesion and then the cell growth.

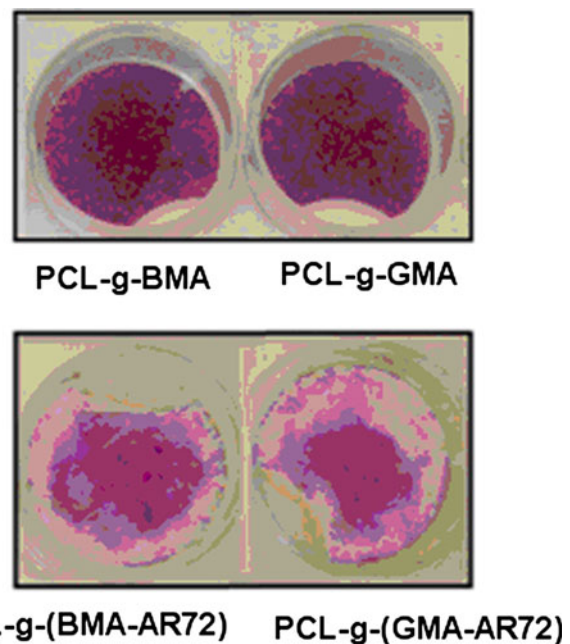


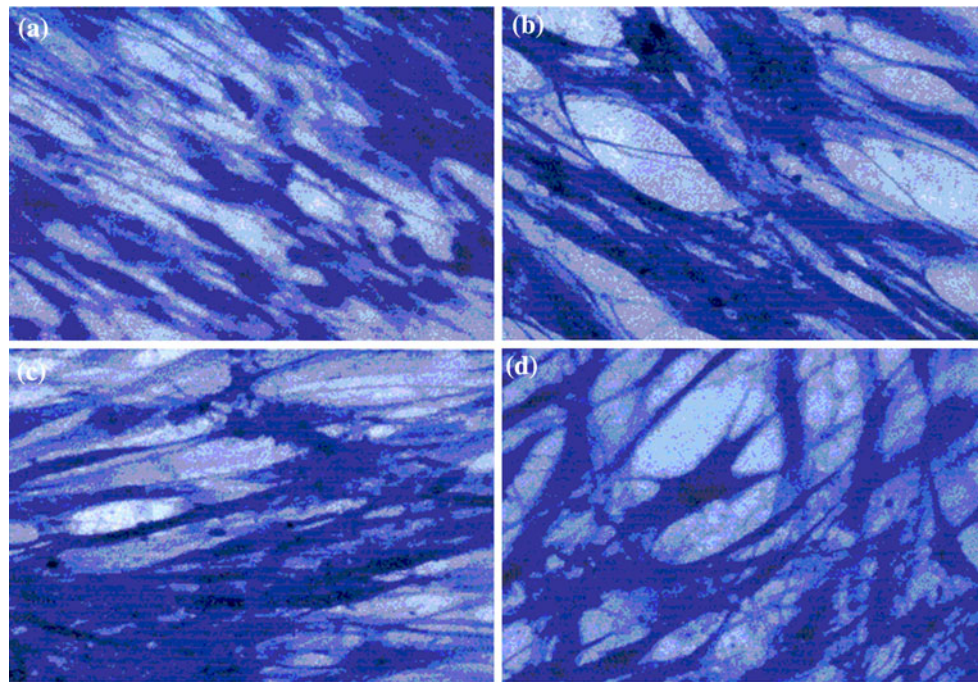
Fig. 8 The macroscopic appearance of some PCL composites after MTT test carried out 7 days after cell seeding

Figure 8 shows the macroscopic appearance of discs of PCL-g-BMA and PCL-g-GMA and of their corresponding biocomposites with functionalized nanosilica AR72. A substantial and regular cell colonization was evident on both PCL-g-BMA and PCL-g-GMA, whereas on their AR72-derivatives composites cells were not only quantitatively lesser but also unevenly distributed.

In addition, crystal violet staining performed in parallel confirmed the minor presence of the cells with respect to composites containing AR72 nanosilica (Fig. 9).

The differentiation of MSCs toward the osteoblastic phenotype is a complex process which follows a precise temporal sequence involving several phases [32]. Alkaline phosphatase (AP), commonly considered an early marker of osteogenic differentiation, is involved in the hydroxyapatite crystal deposition and hence in mineralization of

Fig. 9 The microscopic appearance of MSCs cultured for 7 days on PCL-g-BMA (a), PCL-g-(BMA-AR72) (b), PCL-g-GMA (c), PCL-g-(GMA-AR72) (d), after crystal violet staining (Magnification 200×)



extracellular collagenic matrix [33]. Osteocalcin is a specific late marker of osteogenic differentiation, representing the major non-collagenic protein of the bone matrix, and is expressed exclusively by cells of osteoblastic lineage. Osteocalcin plays a central role in bone mineralization and calcium ion homeostasis. A recent fascinating study has demonstrated that this molecule can be actually considered a hormone by which skeleton exerts a feedback endocrine regulation of energy metabolism [34, 35].

Therefore, to analyze the influence of the various materials on MSCs' differentiative pattern, the expression of the early and late osteoblastic markers, namely AP (Fig. 10a) and OC (Fig. 10b), at 7 and 14 days of culture, respectively, was assessed.

It was evident that PCL-g-BMA expressed the maximum value of alkaline phosphatase activity compared to PCL control, whereas its derivative composite PCL-g-(BMA-AR72) exhibited values markedly lower. This

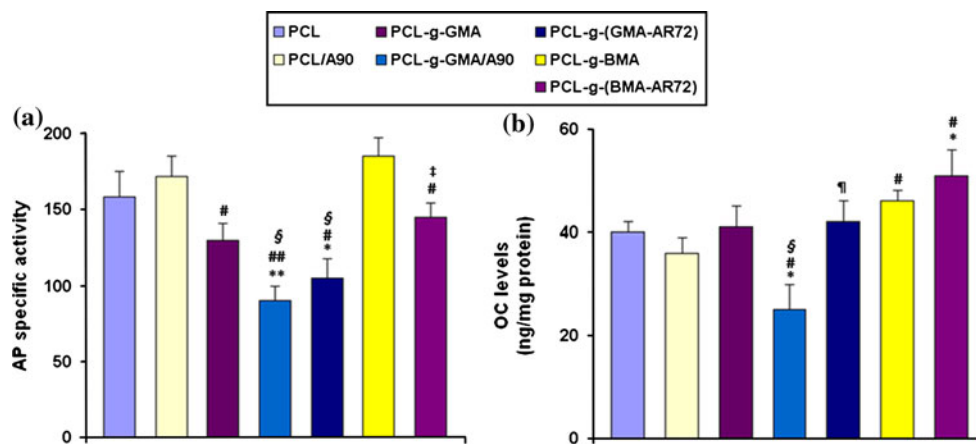


Fig. 10 a Alkaline phosphatase specific activity of stromal cells cultured for 7 days on PCL (control) and its new derivatives and composites. **b** Osteocalcin synthesis 2 weeks after MSCs' plating on PCL (control) and its new derivatives and composites. The last 3 days the cells were incubated in FCS-free Opti-MEM in presence of 0.1%

bovine serum albumin and 100 nM 1,25-dihydroxycholecalciferol. $p < 0.05$ and $** p < 0.01$ versus PCL; $\# p < 0.05$ and $## p < 0.01$ versus PCL/A90; $\$ p < 0.05$ versus PCL-g-GMA; $p < 0.05$ versus PCL-g-GMA/A90; $\ddagger p < 0.05$ versus PCL-g-BMA

decrease was evident also in the case of PCL-g-GMA and PCL-g-(GMA-AR72).

On the contrary, the osteocalcin synthesis by MSCs cultured on both BMA- and GMA-derivatives composites exhibited values generally higher than PCL. In particular, it is to underline that high OC levels were shown by cells grown on the AR72-composites, and particularly on BMA AR72, whereas low OC levels were found in response to A90-composites, and particularly to GMA-A90 (Fig. 10a and b).

3.4 PCL-g-(BMA-AR72)/PLLA system

Even if the addition of nanoparticles improves the toughness and rigidity of the plain polymer, PCL-based nanocomposites still show mechanical characteristics that are not compatible with their use as bone substitutes in tissue regeneration. PCL is a soft, low Tg polymer, and as such is used mainly for controlled drug delivery. The addition of PLLA to the PCL-based nanocomposites could be beneficial in terms of mechanical properties. PLLA is a hard semicrystalline polymer, with a biodegradation rate compatible with bone regeneration, and it has been widely reported in tissue engineering applications. A preliminary screening on the influence of the addition of different amounts of PLLA to PCL/silica nanocomposites has been performed. On the basis of reported biological evaluations, the PCL-g-(BMA-AR72) 3% composite was selected for the preparation of blends with PLLA. Three compositions have been considered, namely, 30:70, 50:50 and 70:30 by weight. Results of MTT test are reported in Fig. 11.

It is evident that the cell viability on PLLA is far less compared to PCL and PCL-g-(BMA-AR72) 3%, and decreases in the blends proportionally to PLLA content.

Fig. 12 The microscopic appearance of MSCs cultured for 4 days on nanocomposites and PLLA blends after crystal violet staining (Magnification 200×)

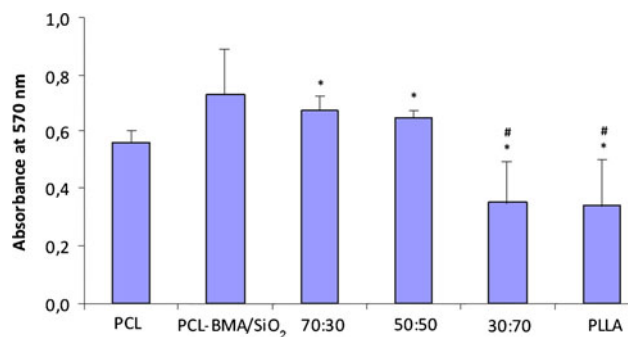
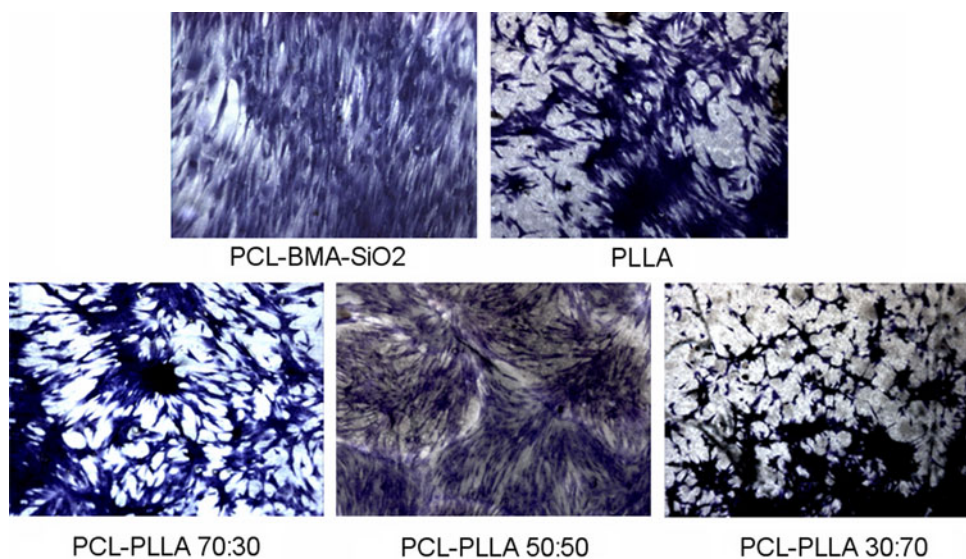


Fig. 11 MTT test carried out after plating 60,000 MSCs onto nanocomposites and PLLA blends for 4 days. * $p < 0.05$ versus PCL; # $p < 0.05$ versus PCL-BMA/SiO₂

Nevertheless, the 70:30 and 50:50 blends still show a higher viability compared to PCL. Crystal violet staining confirmed the minor presence of cells on PLLA and 30:70 formulation with respect to plain PCL and PCL-nanocomposite (Fig. 12).

Finally, the expression of AP and OC markers was assessed. It is evident that the maximum of AP specific activity was exhibited by 70:30 blend and that the increasing presence of PLLA slightly decreased this parameter which was nevertheless higher than PCL and its nanocomposite for all the three blends (Fig. 13a). In contrast the plain PLLA showed the lowest value that was 50% with respect PCL and its nanocomposite and about 35% with respect 70:30 blend.

An opposite finding was evidenced for OC levels, that for 70:30 blend were included between plain PCL and its nanocomposite and progressively increased with PLLA addition. The highest OC levels were detected with 30:70 blend while a OC value comparable to both nanocomposite and 50:50 formulation was found with pure PLLA (Fig. 13b).

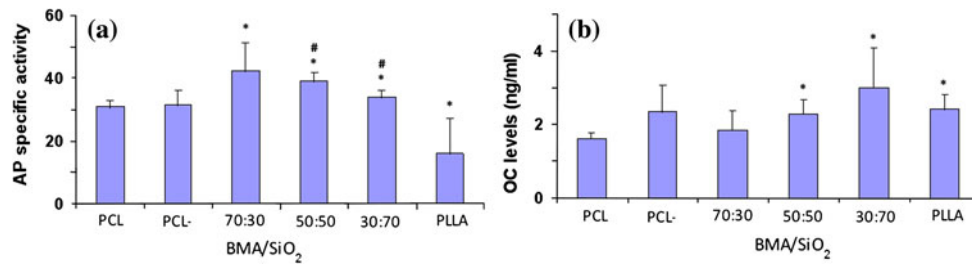


Fig. 13 a Alkaline phosphatase specific activity of stromal cells cultured for 4 days on PCL (control) and its nanocomposite and PLLA blends. **b** Osteocalcin synthesis 7 days after MSCs' plating on PCL (control) and its nanocomposite and PLLA blends. The last

3 days the cells were incubated in FCS-free Opti-MEM in presence of 0.1% bovine serum albumin and 100 nM 1,25-dihydroxycholecalciferol. * $p < 0.05$ versus PCL; # $p < 0.05$ versus PCL-BMA/SiO₂

4 Conclusion

In this article we reported the preparation and characterization of new nanocomposites based on polycaprolactone reinforced with nanostructured silica, projected for biomedical applications in orthopaedic, maxillo-facial and dental surgery fields.

The chemical modification of the PCL, necessary to realize a stable interface with the nanosilica, has been carried out directly in the processing equipment and has allowed to increase the mechanical characteristics of the polyester without worsening its biocompatibility characteristics. The characterization of mechanical properties performed on the new nanocomposites has demonstrated an increase of rigidity of the material without compromising the tenacity.

In particular, Young's modulus was increased to a level by far superior to the neat PCL. The mechanical properties reflect the morphology of the materials, analyzed by means of SEM, where an interfacial adhesion was clearly evidenced as a consequence of the chemical modification. In conclusion, the improvement of mechanical properties of the nanocomposites compared with the pure PCL can allow their potential use as scaffolds or membrane barriers.

In vitro the biocompatibility of these novel biocomposites as well as their capacity to induce the osteogenic differentiation of human bone marrow stromal cells was investigated. In particular we analyzed the adhesion and the growth of these cells, being the contact with the material crucial for all the following events, including the expression of biochemical specific markers, namely alkaline phosphatase and osteocalcin. None of new PCL-silica nanocomposites exhibited cytotoxicity, on the contrary the cells adhered and grew onto all the materials even if at different extent.

Overall, at the basis of the biological as well as the mechanical results, the novel nanocomposites, in particular the one based on PCL-g-BMA, appear promising for bone tissue engineering applications.

A preliminary investigation on materials based on blends between PLLA and the PCL-g-BMA based nanocomposite showed that a further improvement is obtained with respect to the plain nanocomposite in terms of biological response (cell adhesion and proliferation; AP and OC expression): in particular, the 50:50 blend appeared to show the best performance. More work is in progress on the mechanical characterization of the blends, at the aim to select the optimal composition for clinical applications.

References

- Lakes R. Materials with structural hierarchy. *Nature*. 1993;361: 511–5.
- Hartgerink JD, Beniash E, Stupp SI. Self-assembly and mineralization of peptide-amphiphile nanofibers. *Science*. 2001;294: 1684–8.
- Webster TJ, Siegel RW, Bizios R. Enhanced functions of osteoblasts on nanophase ceramics. *Biomaterials*. 2000;21:1803–10.
- Webster TJ, Ergun C, Doremus RH, Siegel RW, Bizios R. Specific proteins mediate enhanced osteoblast adhesion on nanophase ceramics. *J Biomed Mater Res*. 2000;51:475–83.
- Webster TJ, Siegel RW, Bizios R. Osteoblast adhesion on nanophase ceramics. *Biomaterials*. 1999;20:1221–7.
- Rhee SH, Choi JY. Preparation of a bioactive polymethyl methacrylate/silica nanocomposite. *J Am Ceram Soc*. 2002;85:1318–20.
- Yang JM, Lu CS, Hsu YG, Shih CH. Mechanical properties of acrylic bone cement containing PMMA-SiO₂ hybrid sol-gel material. *J Biomed Mater Res Appl Biomater*. 1997;38:143–54.
- Wei Y, Jin D. A new class of organic-inorganic hybrid dental materials. *Polym Prep*. 1997;38:122–3.
- Paul PP, Timmons SFW, Machowski J. Organic-inorganic hybrid dental restorative composites. *Polym Prep*. 1997;38:124–5.
- Rhee SH. Effect of calcium salt content in the poly-ε-caprolactone/silica nanocomposite on the nucleation and growth behavior of apatite layer. *J Biomed Mater Res A*. 2003;67:1131–8.
- Yoo JJ, Rhee SH. Evaluations of bioactivity and mechanical properties of poly(ε-caprolactone)/silica nanocomposite following heat treatment. *J Biomed Mater Res A*. 2004;68: 401–10.
- Wei J, Heo SJ, Liu C, Kim DH, Kim SE, Hyun YT, Shin JW, Shin JW. Preparation and characterization of bioactive calcium silicate and poly(ε-caprolactone) nanocomposite for bone tissue regeneration. *J Biomed Mater Res A*. 2009;90:702–12.

13. Xu T, Zhang N, Nichols HL, Shi D, Wen X. Modification of nanostructured materials for biomedical applications. *Mater Sci Eng C*. 2007;27:579–94.
14. Qhobosheane M, Santra S, Zhang P, Tan WH. Biochemically functionalized silica nanoparticles. *Analyst*. 2001;126:1274–8.
15. Moghimi SM, Hunter AC, Murray JC. Long-circulating and target-specific nanoparticles: theory to practice. *Pharmacol Rev*. 2001;53:283–318.
16. Xu H, Yan F, Monson EE, Kopelman R. Room-temperature preparation and characterization of poly ethylene glycol-coated silica nanoparticles for biomedical applications. *J Biomater Res A*. 2003;66:870–9.
17. Butterworth MD, Illum L, Davis SS. Preparation of ultrafine silica- and PEG-coated magnetite particles. *Colloids Surf A: Physicochem Eng Aspects*. 2001;179:93–102.
18. Li S, Shah A, Hsieh AJ, Haghghat R, Solomon Praveen S, Mukherjee I, Wei E, Zhang Z, Wei Y. Characterization of poly(2-hydroxyethyl methacrylate)-silica hybrid materials with different silica contents. *Polymer*. 2007;48:3982–9.
19. Friedenstien AJ, Chailakhyan RK, Gerasimov UV. Bone marrow osteogenic stem cells: in vitro cultivation and transplantation in diffusion chambers. *Cell Tissue Kinet*. 1987;20:263–72.
20. Prockop DJ. Marrow stromal cells as stem cells for nonhematopoietic tissues. *Science*. 1997;27:671–4.
21. Pittenger MF, Mackay AM, Beck SC, Jaiswal RK, Douglas R, Mosca JD, Moorman MA, Simonetti DW, Craig S, Marshak DR. Multilineage potential of adult human mesenchymal stem cells. *Science*. 1999;284:143–7.
22. Toma C, Pittenger MF, Cahill KS, Byrne BJ, Kessler PD. Human mesenchymal stem cells differentiate to a cardiomyocyte phenotype in the adult murine heart. *Circulation*. 2002;105:93–8.
23. Kopen GC, Prockop DJ, Phinney DG. Marrow stromal cells migrate throughout forebrain and cerebellum and they differentiate into astrocytes after injection into neonatal mouse brains. *Proc Natl Acad Sci USA*. 1999;96:10711–6.
24. Woodbury D, Schwarz EJ, Black IB, Prockop DJ. Adult rat and human bone marrow stromal cells differentiate into neurons. *Neurosci Res*. 2000;61:364–70.
25. Seshi B, Kumar S, Sellers D. Human bone marrow stromal cell: coexpression of markers specific for multiple mesenchymal cell lineages. *Blood Cells Mol Dis*. 2000;26:234–46.
26. Herzog EL, Chai L, Krause DS. Plasticity of marrow-derived stem cells. *Blood*. 2003;102:3483–93.
27. Oliva A, Passaro I, Di Pasquale R, Di Feo A, Criscuolo M, Zappia V, Della Ragione F, D'Amato S, Annunziata M, Guida L. Ex vivo expansion of bone marrow stromal cells by platelet-rich plasma: a promising strategy in maxillo-facial surgery. *Int J Immunopathol Pharmacol*. 2005;18:47–53.
28. Zhang R, Ma PX. Porous poly(L-lactic acid)/apatite composites created by biomimetic process. *J Biomed Mater Res*. 1999;45:285–93.
29. Reverchon E, Pisanti P, Cardea S. Nanostructured PLLA/hydroxyapatite scaffolds produced by a supercritical assisted technique. *Ind Eng Chem Res*. 2009;48:5310–6.
30. Stöber W, Fink A, Bohn E. Controlled growth of monodisperse silica spheres in the micron size range. *J Colloid Interf Sci*. 1968;26:62–9.
31. Friedenstien AJ, Deriglasova UF, Kulagina NN, Panasuk AF, Rudakowa SF, Luria EA, Ruadkow IA. Precursors for fibroblasts in different populations of hematopoietic cells as detected by the in vitro colony assay method. *Exp Hematol*. 1974;2:83–92.
32. Lian JB, Stein GS. Concepts of osteoblast growth and differentiation: basis for modulation of bone cell development and tissue formation. *Crit Rev Oral Biol Med*. 1992;3:269–305.
33. Majeska RJ, Rodan GA. The effects of 1,25OH₂D₃ on alkaline phosphatase in osteoblastic osteosarcoma cells. *J Biol Chem*. 1982;257:3362–7.
34. Harada S, Rodan GA. Control of osteoblast function and regulation of bone mass. *Nature*. 2003;423:349–55.
35. Lee NK, Sowa H, Hinoi E, Ferron M, Ahn JD, Confavreux C, Dacquin R, Mee PJ, McKee MD, Jung DY, Zhang Z, Kim JK, Mauvais-Jarvis F, Ducy P, Karsenty G. Endocrine regulation of energy metabolism by the skeleton. *Cell*. 2007;130:456–69.